J. Physiol. (1977), **272**, *pp.* 1–23
With 5 plates and 8 text-figures
Printed in Great Britain

MORPHOLOGY AND RESPONSES TO LIGHT OF THE SOMATA, AXONS, AND TERMINAL REGIONS OF INDIVIDUAL PHOTORECEPTORS OF THE GIANT BARNACLE

BY A. J. HUDSPETH* AND ANN E. STUART

From the Department of Neurobiology, Harvard Medical School, Boston, Massachusetts 02115, and the Division of Biology, California Institute of Technology, Pasadena, California 91125, U.S.A.

(*Received 5 October 1976*)

SUMMARY

1. The median eye of the giant barnacle, *B. nubilus*, comprises four large photoreceptor neurones which are visible under the dissecting microscope for almost their entire length. We have studied the structure of, and the responses to light recorded in, the somata, axons, and terminal regions of these neurones.

2. The photoreceptor somata, each 40–70 μm in diameter, extend numerous light-sensitive dendritic processes whose membranes form rhabdomeric microvilli. Recordings from the soma show that dim light evokes a steady, noisy depolarization; brighter light elicits a transient depolarization which decays to a maintained plateau, followed by a hyperpolarization when the light is turned off.

3. Light-induced voltage changes spread decrementally along the photoreceptor axons, which average 10 mm in length and 25 μm in diameter. In distal parts of the axon, near the presynaptic terminals, depolarizations and hyperpolarizations can be as large as 50 % or more of their values in the soma.

4. There is no demonstrable electrical coupling between photoreceptor neurones as shown by simultaneous recordings from two receptor somata or axons.

5. Each photoreceptor axon enters the mid line commissure of the supraoesophageal ganglion, bifurcates, and arborizes in a restricted zone of neuropil in each hemiganglion. The large size of the terminal processes of these neurones and their characteristic cytoplasmic inclusions enable one to trace them with the electron microscope as they branch in the neuropil.

* Present address: Division of Biology, California Institute of Technology, Pasadena, California 91125, U.S.A.

6. The terminal processes subdivide and end in 1–3 μm diameter branches which are the sites of apparently chemical synapses. Vesicle-containing, presynaptic loci on these processes of the receptor cell are invariably apposed to two post-synaptic processes from cells as yet unidentified.

INTRODUCTION

Photoreceptors of vertebrates and invertebrates can respond to minute changes in light intensity over a wide dynamic range, converting these intensity differences to changes in membrane potential. The resulting potential fluctuations in the receptor neurone can be as small as fractions of a millivolt, yet can affect higher-order neurones (Hagins, Penn & Yoshikami, 1970; Shaw, 1972; Schwartz, 1974, 1975). Such capabilities focus interest on the processes of transmission of visual signals along the axon of the receptor cell and from its presynaptic terminals to post-synaptic cells. These processes are poorly understood, in part because the photoreceptors of the vertebrate retina or arthropod compound eye, whose light-receptive properties and anatomical connexions with post-synaptic cells are well known, are usually too small and too densely packed to permit direct study of their axons and synaptic regions.

The photoreceptors of barnacles (Cornwall, 1953; Gwilliam, 1963, 1965; Fahrenbach, 1965) offer advantages of size and accessibility which invite study of the properties of their axons and terminals. In several barnacle species, the photoreceptors have large cell bodies and axons, and are unusually few in number. Their cell bodies lie peripherally, grouped in simple eyes called ocelli, and they entend long axons to innervate cells in the supraoesophageal ganglion of the central nervous system. The visual signal is initiated in dendritic extensions of the cell body and is transmitted decrementally to the cell's synaptic region within the ganglion (Gwilliam, 1963; Shaw, 1972; Millecchia & Gwilliam, 1972; Hudspeth, Poo & Stuart, 1977). In the central nervous system, light changes initiate a simple 'shadow reflex' behaviour; the animal responds to the dimming of ambient light, such as occurs when a predator passes overhead and casts a shadow, by withdrawing into its shell and closing its opercular plates (Gwilliam, 1963).

One species of barnacle, the giant Pacific barnacle, *Balanus nubilus*, has the great advantage that one can see under a dissecting microscope the entire length of the receptor cells of the median ocellus. In addition it is possible to see individual cells of the supraoesophageal ganglion including neurones which may be directly contacted by the receptor cells (Ozawa, Hagiwara, Nicolaysen & Stuart, 1976). In the work presented here, we have studied the morphology of the somata, axons, and terminal regions of individual photoreceptors, and have recorded intracellularly the physio-

logical responses to light all along the cell. In the accompanying paper we examine the properties of the receptor cell which appear responsible for the transmission of visual signals from the soma to the synaptic terminals.

METHODS

General

Giant barnacles (*Balanus nubilus* Darwin) from Puget Sound were supplied by Mr Cleave Vandersluys and Mr David King (Friday Harbor, Washington). Animals of a wide range of sizes were used in experiments; all the reported physiological results were obtained with animals measuring about 40 mm across their opercular openings, while the anatomical studies employed barnacles 20–30 mm in that dimension. The barnacles, which were maintained at 11 °C in filtered, aerated sea water in a recirculating tank, showed normal feeding movements and withdrawal reflexes for at least several months.

Dissections and experiments were carried out, unless otherwise stated, in a physiological saline solution containing 462 mM-NaCl, 8 mM-KCl, 20 mM-$CaCl_2$, 12 mM-$MgCl_2$, and 10 mM-Tris (hydroxymethyl) aminomethane-HCl buffer at pH 7·7 (Brown, Hagiwara, Koike & Meech, 1970).

Animals were removed from the basal portions of their shells by cutting the tendinous attachments between the fixed and opercular plates and removing the body mass, still attached to the operculum, by reaching deep within the shell and sectioning the retractor musculature. The opercular plates were immobilized, external aspect downwards, by wedging the shell firmly beneath large needles and against the waxed bottom of a dish. The remaining cuticle surrounding the oesophagus and the thin membrane overlying the scutal adductor muscle were then carefully cut along the mid line. Subsequent dissection of the thin layers of muscle overlying the gut exposed the median ocellus, its nerve, and the supraoesophageal ganglion in which the nerve terminates. These structures were then either fixed for anatomical observation or removed for physiological experiments as described below.

Anatomy

The structures of interest were fixed *in situ* by dripping fixative at 0–11 °C on the partially dissected preparation at a rate of 1–2 ml./min for 5 min. The ocellus, its nerve, and the ganglion were then freed and the preparation immersed in fixative for a further 30–90 min at the same temperature.

Of a variety of phosphate and cacodylate-buffered fixative solutions tried, the most successful contained 250 mM glutaraldehyde, 510 mM-NaCl, 90 mM sucrose, and 100 mM sodium phosphate buffer. This mixture had a pH of 7·4 and a total osmolality of 1050 m-osmole/kg.

Following primary fixation, preparations for electron microscopy were transferred without a wash to a postfixative solution at 0–2 °C; post-fixation was generally for 60–90 min. The standard solution consisted of 30 mM osmium tetroxide and 80 mM glutaraldehyde in the buffered medium above.

Procion yellow-injected specimens were fixed for 15 min at pH 4·0 and room temperature in 650 mM formaldehyde, 510 mM-NaCl, 90 mM sucrose, 5 mM-$CaCl_2$, and 120 mM sodium cacodylate buffer.

The terminal regions of single receptors were traced with precipitate of cobalt ion as follows. Individual receptor axons were partially teased from the ocellar nerve and their cut ends immersed in a pool of $CoCl_2$ hypotonic (350 mM) to barnacle

saline. The cobalt diffused along the 3–4 mm stump of axon in 3–4 hr. The preparation was fixed for 15 min in the cacodylate-buffered mixture above at pH 7·4; cobaltous ion was then precipitated with 1% ammonium sulphide in saline. After dehydration, specimens were cleared in amyl acetate and examined as whole mounts in Lustrex HF55-2020 (Monsanto). Precipitation of cobaltous sulphide before fixation resulted in artifactual swelling of filled processes.

All specimens were dehydrated in graded ethanol solutions and passed through propylene oxide before embedding. Light microscopic preparations, including fluorescent specimens, were embedded in a soft epoxy plastic mixture (Kushida, 1971), while electron microscopic material was placed in a standard hard Epon (Luft, 1961).

Sections for light microscopy were cut on glass knives at thicknesses of 0·5–2 μm, except for fluorescent preparations which were cut at 5–10 μm. Light microscopic sections were stained with 1% toluidine blue in Na borate buffer. Electron microscopic sections were cut on a diamond knife and had silver to grey interference colours. They were collected on uncoated grids, stained with aqueous uranyl acetate and lead citrate (Venable & Coggeshall, 1965), and examined with a Philips EM 200 or EM 301G operated at 80 kV.

Living preparations were immobilized with spring clips in a glass-bottomed, saline filled chamber (McMahan & Kuffler, 1971) and photographed with darkfield or Nomarski differential interference optical systems. Methylene blue preparations were examined by the same technique after staining with 0·003% dye in barnacle saline solution.

Physiology

After preliminary dissection as described above, the median ocellus and its nerve were cut free from the surrounding connective tissue, the muscle accompanying the ocellar nerve was sectioned, and the supraoesophageal ganglion was removed by sectioning its other nerves (leaving long stumps of the circumoesophageal connectives for drawing into suction electrodes).

Each preparation was placed in a flat-bottomed, roughly 1 ml. chamber lined with Sylgard 184 plastic (Dow Corning), and held in place with pins of 50 μm diameter wire inserted through connective tissue around the ganglion, nerves, and ocellus. The folded ocellar nerve was straightened and secured at intervals along its length by pinning across it pieces of nerve taken from elsewhere in the animal; this procedure provided stability for recording from receptor axons. Recordings from photoreceptor axon terminals were most easily obtained with the ganglion pinned dorsal side uppermost.

To facilitate micro-electrode penetrations, the preparation was placed for 3 min at room temperature in collagenase 3 mg/ml. (Sigma, Type 1 from *Clostridium histolyticum*, specific activity 260 units/mg). In some experiments, pronase 0·5 mg/ml. (CalBiochem, B grade) was added to the collagenase. This enzymic procedure caused no obvious changes in the ultrastructure of the photoreceptor cells or ganglionic constituents, although the structure of the collagen sheath was disrupted. Ganglion cells showed similar physiological properties whether penetrated after enzyme treatment or after they had been exposed by sheath dissection. Following a thorough washout of the enzymes, the preparation was superfused steadily throughout experiments at 20–24 °C.

The experimental chamber was fixed on a stage in a light-tight box. Substage illumination for preliminary manipulations was provided by a long-working-distance darkfield condenser and microscope illuminator. After stable electrode penetrations were achieved, white light stimuli, unfiltered with respect to wavelength, were delivered through a fibre-optics cable whose tip was positioned 7·5 cm above the preparation. The divergent cone of light from the fibre-optics illuminated

the preparation uniformly; however, the light must have been scattered and attenuated to a certain degree by the connective tissue overlying the cells. The light source was a quartz-halogen lamp (Labsource QH-150, PBL International) equipped with a set of neutral-density filters and an electromagnetic shutter (Vincent Associates) with a 4 msec opening and closing time. To minimize adaptation to the preceding light during a series of measurements, stimuli of greater irradiance than $10^{-4 \cdot 8}$ times the maximum were separated by at least 2–5 min, and by longer intervals if needed for the membrane to recover from post-illumination hyperpolarization. The absolute energy of the unattenuated stimulus was determined with a light measuring instrument equipped with a radiometric filter (Model 40X, United Detector Technology) and placed in the position of the preparation. The maximal irradiance was 1·3 mW/cm^2.

Cells were penetrated with micro-electrodes (60–100 MΩ) filled with 4 M potassium acetate. Procion yellow M4-RAN was injected with similar electrodes of approximately 400 MΩ resistance when filled with a 6% solution. To penetrate receptor somata and axons, the tip of the electrode first had to be driven through the several layers of loosened capsule by light tapping on the manipulator. Penetrations of the axons were easiest near points at which the nerve had been secured. Conventional techniques of intracellular recording and stimulation were used. Applied current was measured through the bath ground by a current-to-voltage converter made from an operational amplifier (Analog Devices 540 J).

During impalement it was usual to encounter cells which had greater resting potentials (−75 to 80 mV) than the receptor cell. Such cells did not give regenerative responses to electrical stimulation and were insensitive to even the brightest light available. Anatomical observations suggest that these recordings may have been made from fibrocytes of the capsule (Fahrenbach, 1965; A. J. Hudspeth, unpublished observations), relatively large and ubiquitous cells which are more likely to be impaled than the slender glial processes ensheathing the receptor. Occasionally a neurone of the same approximate size as a photoreceptor could be seen under the dissecting microscope in association with the ocellus. This neurone had a resting potential of −50 to −60 mV, gave overshooting action potentials, and was insensitive to light.

RESULTS

The central nervous system of *Balanus nubilus* is typical of those of most barnacles in that it consists of two bilaterally symmetrical ganglia, one located dorsal and the other ventral to the oesophagus, joined by paired circumoesophageal nerve bundles termed connectives (Cornwall, 1953). The supraoesophageal ganglion (Pl. 1*A*) receives input from the axons of primary photoreceptors whose cell bodies are located in three ocelli: a pair of lateral ocelli situated under the shell, and a single median ocellus accessible to light when the animal opens its opercular plates. Visual information from all three ocelli is processed in the supraoesophageal ganglion, and travels via the circumoesophageal connectives to the ventral ganglion where, in experiments on a related species, it has been shown to influence the firing of motor neurones (Gwilliam & Bradbury, 1971; Gwilliam, 1976).

The median ocellus, a spherical mass 100–250 μm in diameter (Pl. 1*A–C*), consists of four co-encapsulated photoreceptor somata embedded in a sheet

of connective tissue between the scutal adductor muscle and the gut. Axons from these photoreceptors, together with several dozen much smaller axons that course past the ocellus, form the median ocellar nerve (Pl. 1*A*, *D*, *E*; Pl. 3*A*). This nerve is usually folded alongside a small muscle to which it is attached (Pl. 3*A*). During the dissection, the muscle is routinely teased away and the median ocellar nerve extended (Pl. 1*A*) for intracellular recording.

Photoreceptor somata of the median ocellus

Morphology. The perikaryal portion of each photoreceptor cell of the median ocellus is slightly prolate, and, in animals of the size used in this study, has a diameter of about 40–70 μm (Pl. 1*B*,*C*). In various specimens, the four cells may be separated from one another or closely packed in a tetrahedral array. In the electron microscope, the cytoplasmic constituents of the somata are unremarkable save for the presence of irregular masses of glycogen particles; the largest aggregates are up to 20 μm in diameter (Pl. 2*A*). Glycogen is also widely distributed in photoreceptor dendritic cytoplasm as single particles and small clusters.

From each of the receptor somata extend numerous, pleiomorphic dendritic processes which are indiscriminately oriented and intertwined with those of the neighbouring receptor cells (Pl. 2*B*). Some dendrites are only about 5 μm in length and 1 μm in diameter (Pl. 2*C*), while others range up to almost an order of magnitude larger in both dimensions (Pl. 2*A*). Dendrites terminate in bulbous or cylindrical swellings about 4–8 μm in diameter packed with mitochondria, lysosomes, and smooth endoplasmic reticulum (Pl. 2*C*). The membrane of the tips of the dendrites is specialized into rhadbomeres consisting of thousands of closely packed microvilli of 1·0–1·7 μm length and 90 nm diameter (Pl. 2*C–E*). Because the rhabdomeres of adjacent cells do not relate to one another in an orderly configuration, there are no true rhabdomes.

Glial cells scattered throughout the ocellus extend thin, lamellar processes which separate many of the photoreceptor dendrites. These cells are rather uniformly 5 μm in perikaryal diameter, and have little cytoplasm about their nuclei (Pl. 2*C*). Their processes, which also contain microtubules and endoplasmic reticulum, are readily identified by their content of numerous mitochondria much smaller than those of the photoreceptor cells. The four receptors are encapsulated by a common connective tissue sheath (Pl. 1*C*; Pl. 2*A*,*B*) about 5 μm in thickness and continuous with the sheath surrounding the ocellar nerve and the supraesophageal ganglion.

Although the elaborate geometry of the photoreceptor dendrites complicates identification of intercellular contacts, an attempt was made to

find any specialized junctions, including synapses, between receptor cells. No such intercellular junctions were observed, although gap junctions and adherent plaques were noted among ocellar glial cells and capsular fibrocytes.

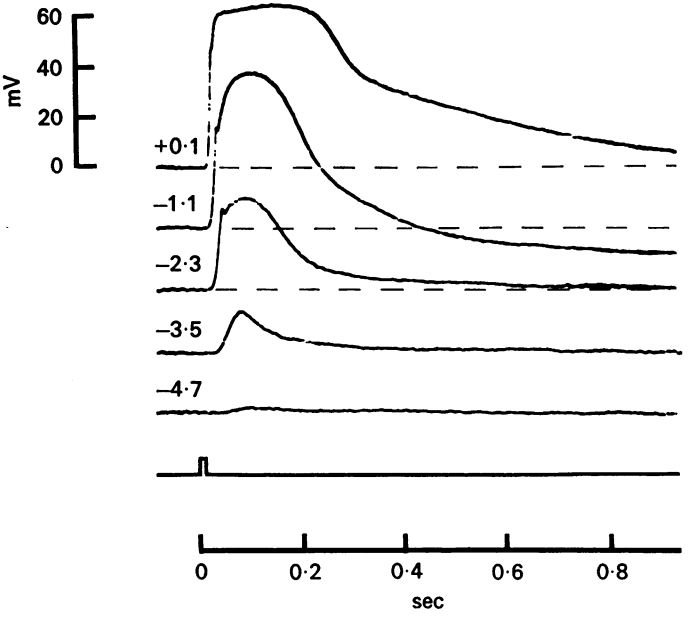

Text-fig. 1. Responses to 10 msec flashes of light recorded from a receptor soma. The records show depolarizations of a receptor from its dark resting potential of -60 mV (interrupted lines) for increasing intensities of light. The log of the irradiance of the light in mW/cm^2 is indicated to the immediate left of each trace. The duration of the light stimulus is indicated by the lowermost trace.

Response of the Soma to light. Text-figs. 1–3 demonstrate various features of the response of the receptor soma to light by showing its responses to flashes, 11 sec pulses, and 1 min periods of illumination. In the dark the cell has a resting potential of -60 mV. Short (10 msec) flashes of light of increasing intensity (Text-fig. 1) elicit from the receptor cell graded, depolarizing responses with latencies that decrease from 65 msec to 5 msec as the intensity of light is increased over five log units. These responses are similar to those observed in other invertebrate receptors, in particular to those of the retinular cells of the honeybee drone (Baumann, 1968). At intensities below $10^{-2\cdot9}$ mW/cm^2, both the rising and falling phases of the response are smooth; brighter stimuli evoke an inflection on the rising phase, and the falling phase of the response also develops at least two components with increasing intensity. Such dramatically different shapes

of the responses at various intensities of illumination suggest that complex processes, probably quite similar to those governing the response of the honeybee photoreceptor (Fulpius & Baumann, 1969; Baumann & Hadjilazaro, 1972), underlie the generation of the barnacle receptor cell response.

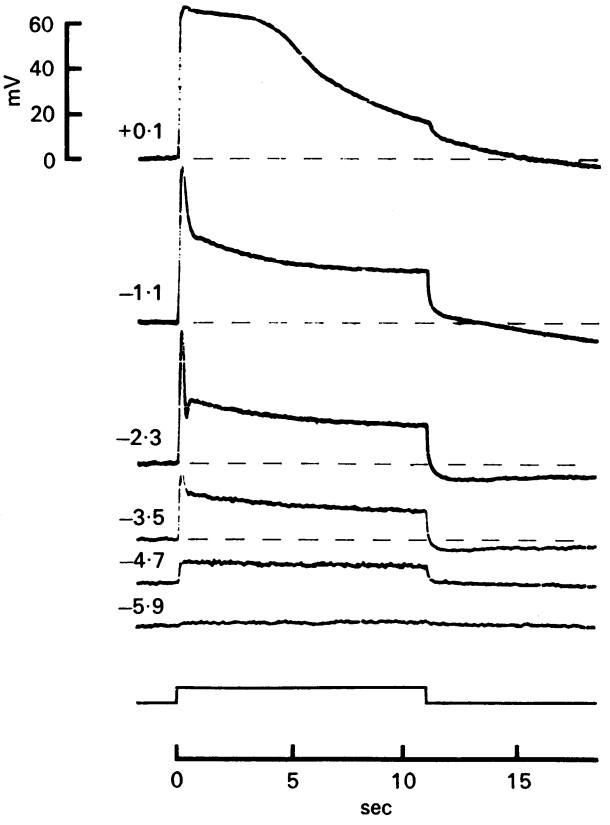

Text-fig. 2. Responses to pulses of light recorded from a receptor soma. The records show depolarizations of the same receptor as in Text-fig. 1 from its dark resting potential of -60 mV (interrupted lines) for increasing intensities of light. The duration and intensity of light are indicated as in Text-fig. 1.

The responses of the receptor soma to longer pulses of light (Text-fig. 2) show how the cell adapts to maintained illumination. Dim lights evoke steady depolarizations which are sustained for the duration of the light. The membrane potential during the responses to dim lights is considerably 'noisier' than in the dark (Hagins, 1965) but discrete potential changes such as are observed in dark-adapted photoreceptors of *Limulus* (Yeandle, 1958; Fuortes & Yeandle, 1964) have not been seen. The noise is not seen

when the cell is depolarized with current; it can be recorded from a light-stimulated receptor cell body even after the ocellar nerve has been severed, which excludes as its cause synaptic feedback from ganglion cells. Consequently it is probably due to discrete responses of the photoreceptor dendrites to dim light. In maintained bright light the response reaches a peak in about 100 msec, then declines with a brief oscillation to a smooth plateau which becomes stable, except in very bright lights, in about 5–10 sec (Text-fig. 2). This decline in the receptor depolarization may be due to an effect of calcium during the light stimulus (Lisman & Brown, 1972; Lisman & Brown, 1975; Bader, Baumann & Bertrand, 1976), since perfusion of the receptors with calcium-free saline causes the peak depolarization to be maintained over time and the response to become 'square'.

The changes in membrane potential resulting when a maintained light is turned off are of particular interest since it is a decrease in light intensity that elicits a behavioural response in the animal (Gwilliam, 1963), and negative-going changes in receptor membrane potential that give rise to impulses in post-synaptic cells (Ozawa *et al.* 1976). The time course and shape of responses recorded in the photoreceptor soma at the termination of illumination are dramatically affected by the duration and intensity of the previous period of illumination, and appear to reflect several different processes initiated by the light. The basic features of this 'off response', and their dependence on intensity, can be seen in Text-fig. 3. At the termination of a 50 sec pulse of dim light the cell remains slightly depolarized, after moderately bright lights ($10^{-3.5}$, $10^{-2.3}$ mW/cm^2) the cell hyperpolarizes, and after bright lights ($10^{-1.1}$, $10^{+0.1}$ mW/cm^2) it remains depolarized initially and then slowly hyperpolarizes.

The negative-going components of the 'off response' include a rapid repolarizing phase resembling the early 'off response' in honeybee retinular cells (Baumann & Hadjilazaro, 1972), and a slow afterpotential, the post-illumination hyperpolarization (Koike, Brown & Hagiwara, 1971). The slow hyperpolarizing afterpotential has been shown to be due to an electrogenic sodium pump in *Limulus* ventral eye (Brown & Lisman, 1972) and in barnacle lateral eye (Koike *et al.* 1971). Both a long-lasting increase in potassium conductance and an electrogenic pump appear to be among the mechanisms governing the shape of the 'off response' in the median receptor of the giant barnacle (D. R. Edgington, personal communication). The amplitude of the post-illumination hyperpolarization in the soma can be remarkable; the intracellular potential has been observed to reach −118 mV following a 10 sec pulse of light of maximal intensity.

Text-fig. 4 presents a plot of the maximum amplitude of the peak depolarization, the amplitude of the plateau at the end of a 10 sec pulse, and the maximum amplitude of the post-illumination hyperpolarization

following the pulse, as a function of light intensity. The dark resting potential of the cell (-60 mV) lies about halfway between the maximal excursions of the membrane potential in response to light and dark (in this case, $+7$ and -98 mV). The initial peak grows non-linearly with the

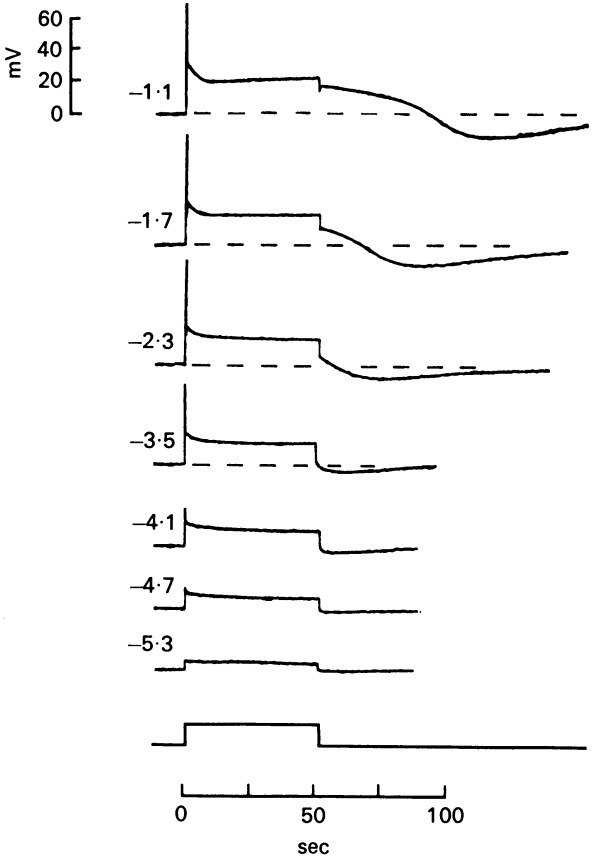

Text-fig. 3. Responses of a receptor soma to a 50 sec period of light followed by a period of dark. Voltage changes are shown as displacements from the dark resting potential of -60 mV (interrupted lines). The duration and intensities of light are indicated as in Text-fig. 1.

logarithm of the light intensity over about 3 log units and saturates at $10^{-1.7}$ mW/cm^2; the plateau depolarization grows roughly in proportion to the logarithm of the light intensity over 6 log units. The post-illumination hyperpolarization also increases approximately linearly with the logarithm of the light intensity; we have not been able to saturate it with the available light.

The median ocellar nerve

Morphology. The axons of the four photoreceptors course together in one of the two compartments of the median ocellar nerve (Pl. 3*A*). Several dozen small fibres compose a second compartment, which is separated by a connective tissue capsule from the first. In some specimens, additional

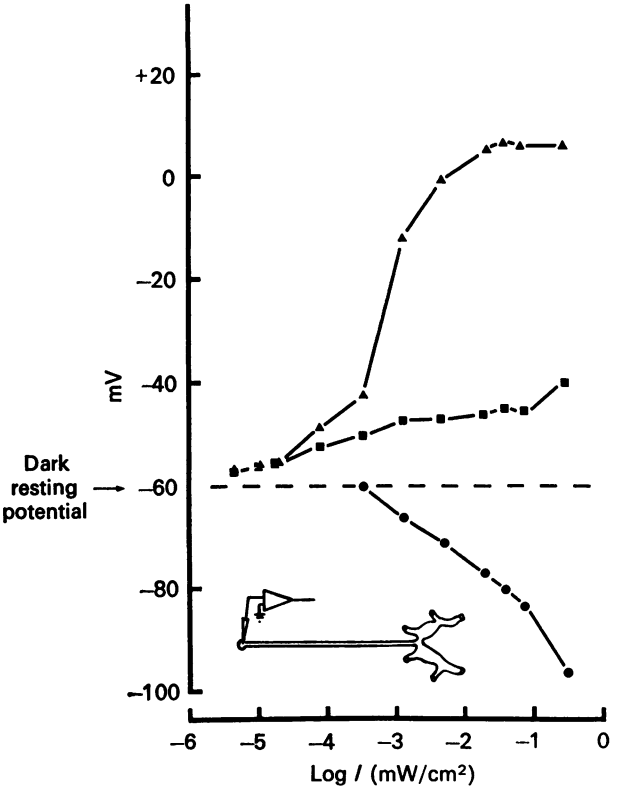

Text-fig. 4. Maximum amplitude of the depolarizing peak (▲), amplitude of the plateau 10 sec after the onset of illumination (■), and maximum amplitude of the post-illumination hyperpolarization (●) in one receptor plotted as a function of log light intensity. Recordings were made from the soma as indicated in the inset diagram. Interrupted line indicates the dark resting potential of −60 mV. The stimulus was 10 sec in duration.

small axons occur in bundles of two or three intercalated within the connective tissue sheaths of the photoreceptor axons but not in direct contact with them. The glial and connective tissue wrapping of the receptor axons is typical of invertebrate peripheral nerves and consists of about ten cytoplasmic lamellae with a total thickness of 0·9 μm or more (Pl. 3*C*).

The diameter of each receptor axon remains rather uniform along the entire length of the ocellar nerve, and ranges from approximately 10 to 40 μm for receptors of 5–15 mm total length. A strong correlation exists between receptor length and axonal diameter (Hudspeth *et al.* 1977).

The median ocellar nerve is closely associated along its entire length with a small strand of striated muscle (Pl. 3*A*,*B*) which extends from the oesophageal musculature to the scutal adductor. The nerve is folded sinuously and attached to the muscle intermittently with connective tissue

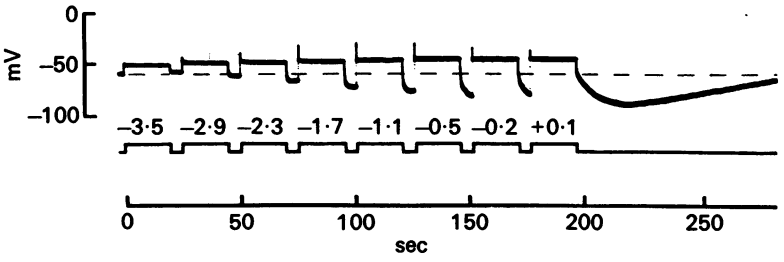

Text-fig. 5. Responses of a receptor axon to 20 sec pulses of light alternating with 5 sec pulses of dark. The electrode was located 75% of the distance from the ocellus to the ganglion. The light pulses, indicated as in Text-fig. 1, increased in intensity from $10^{-3\cdot5}$ to $10^{+0\cdot1}$ mW/cm^2. After the last pulse of light the post-illumination hyperpolarization reached its maximum value at -90 mV. The dark resting potential (-60 mV) is indicated by the interrupted lines.

strands. The ocellar nerve must extend much further when the animal protrudes its body mass to feed than when the body is curled up at rest; the muscle perhaps serves to take up slack in the long nerve to prevent its possible entanglement.

Responses to pulses of light recorded from the axon. A receptor axon can be penetrated anywhere along its length with one or more micro-electrodes. The amplitudes of the peak, plateau, and post-illumination hyperpolarization recorded from the axon are substantial fractions of those recorded from the cell body.

In distal parts of the axon, the post-illumination hyperpolarization can dominate the response. In the experiment of Text-fig. 5, an electrode was placed in an axon at a point 75% of the distance from the ocellus to the commissure, and the cell was stimulated with 20 sec pulses of light of increasing intensity interrupted by 5 sec pulses of dark. (Note that the initial peak depolarization in Text-fig. 5 reaches -30 mV at intensity $10^{-1\cdot1}$ mW/cm^2, but becomes smaller at higher intensities because of adaptation to the preceding light.) The main point is that steady illumination does not depolarize the cell in this case beyond about -45 mV,

even in bright light, whereas the post-illumination hyperpolarization during the pulses of dark continues to grow, developing maximum of −90 mV after the brightest light pulses. Hyperpolarization of the axon to −97 mV has been observed 0·35 mm from the terminal arborization of a 10·5 mm long receptor.

Terminations of the receptors in the supraoesophageal ganglion

Morphology. In most preparations, at least one or two of the four photoreceptor axons can be clearly seen under the dissecting microscope as they enter the supraoesophageal ganglion at the mid line of its commissure, bifurcate, and send large processes to each hemiganglion (Pl. 1*F*). The structural details of the terminations of single receptors have been demonstrated by a variety of techniques including intracellular injection of Procion yellow dye, diffusion and precipitation of cobalt ion in single dissected receptor axons, methylene blue staining of whole nerves, and light and electron microscopy of serial sections. All of these techniques give consistent results. Each photoreceptor axon divides one to several times as the ocellar nerve inserts into the ganglionic commissure (Pl. 1*G*) and sends at least one branch into each side of the ganglion (Pl. 4*A*,*B*; Text-fig. 6). Some axons make only a single, Y- or T-shaped division within the commissure; others begin sequential branching within the ocellar nerve several hundred micrometers from the commissure, and produce multiple terminal processes. However, in every case the arborization is restricted to a defined zone of neuropil near the junction of the commissure with the hemiganglion.

In the commissure the terminal branches of the four photoreceptor axons, their number dependent upon the number of axonal bifurcations, run parallel with and adjacent to one another along the (anterior) aspect of the commissure from which the nerve enters (Pl. 4*C*,*D*). They terminate in the ganglionic neuropil by extensive arborization at a distance of about 100 μm from the commissural mid line (Pl. 4*A*,*B*; Text-fig. 6). The photoreceptor terminals and related processes in each half of the ganglion occupy a distinct, roughly cylindrical portion of the neuropil which can be recognized in parasagittal sections.

The terminal processes of the photoreceptor cells are readily recognized in electron micrographs from several characteristic features: they run in the commissure on the side opposite the much larger bundle of decussating fibres (Pl. 4*C*), they are large, and their cytoplasm contains numerous glycogen particles (Pl. 4*D*). The axon terminals contain microtubules, neurofilaments, mitochondria, and membrane vesicles (Pl. 5*A*). As they extend into the neuropil, the terminals decrease in diameter by successive branchings; small branches of roughly 1–3 μm diameter (Pl. 5*A*,*B*) are the

sites of apparently chemical synapses. These terminals contain clusters of 60 nm, membrane-bounded vesicles surrounding dense structures in the presynaptic cytoplasm, and are invariably apposed to two post-synaptic processes of roughly 0·5 μm diameter (Pl. 5*C*). The presynaptic dense bodies are of a homogeneous texture and about 100 nm in diameter. Both the pre- and post-synaptic membranes are characteristically lined with cytoplasmic densities. The terminals of photoreceptor cells have not been seen to form gap junctions or to receive synapses from other cells.

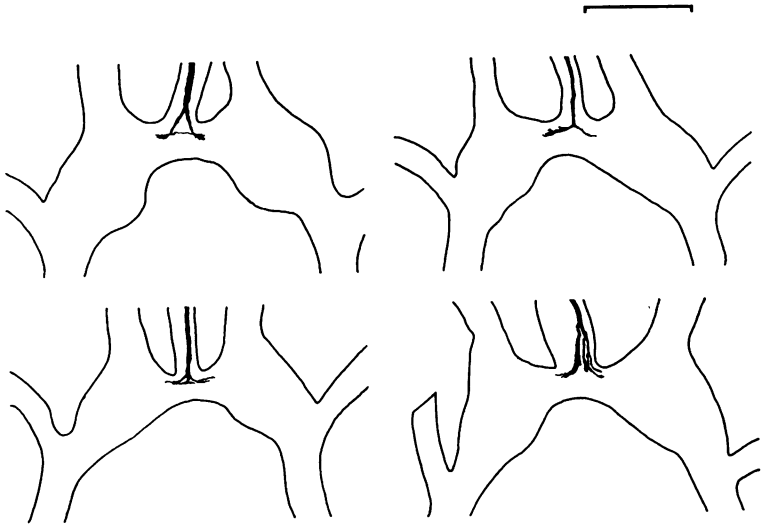

Text-fig. 6. Camera lucida drawings of the terminations of individual median ocellar photoreceptor axons in supraoesophageal ganglia. The upper left preparation was stained by the methylene blue technique, the others by diffusion of cobalt ion along single, teased axons and precipitation of the dense sulphide after fixation. Despite the wide variability in the complexity of branching, the positions and extent of the terminals are similar from animal to animal. Scale, 500 μm.

Physiology. The axon of a photoreceptor neurone can be impaled easily at any point up to its bifurcation. With somewhat more difficulty one can also record from the smaller receptor cell process in the commissure beyond the bifurcation. Text-fig. 7 shows a series of responses to 10 sec pulses of increasing light intensity recorded from a branch of an 8 mm long receptor axon after its bifurcation and entry into the commissure. The terminal depolarizes and hyperpolarizes by tens of millivolts in response to light and dark. In such terminal recordings the size of the peak depolarization is decreased compared to those of the plateau and post-illumination hyperpolarization.

In the terminal recording of Text-fig. 7, a marked hyperpolarization transiently interrupts the slow falling phase following a pulse of unattenuated light (compare with the repolarizations following the responses to the brightest lights presented in Text-figs. 2 and 3). This transient hyperpolarization is characteristic of the terminal region and will be dealt with in a later paper.

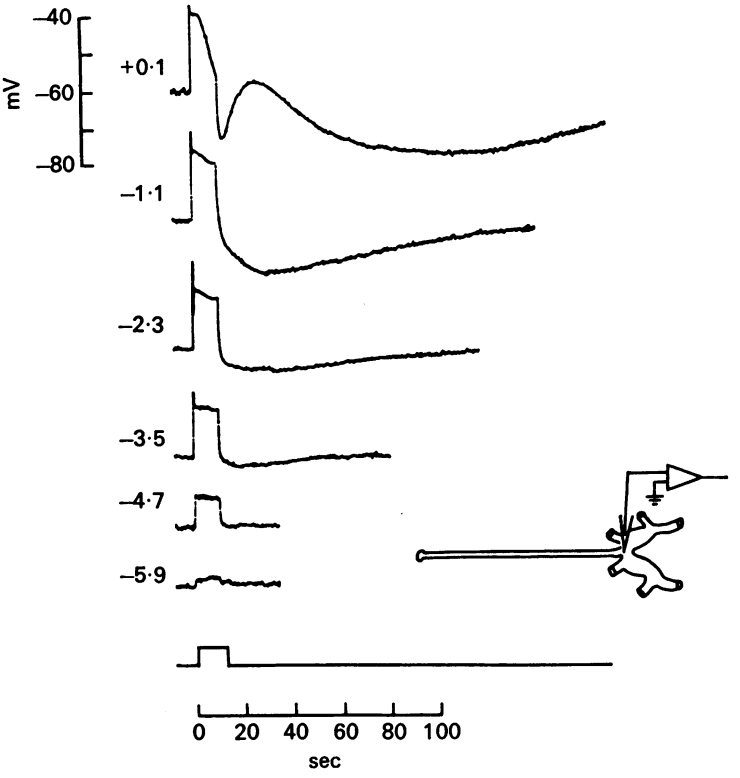

Text-fig. 7. Responses of a receptor terminal branch within the commissure of the supraoesophageal ganglion, as shown in the inset diagram. Responses to increasing light intensities are shown as displacements from a resting potential of -60 mV. The duration and intensities of light are indicated as in Text-fig. 1. The total receptor length was 8·0 mm. At intensity $10^{-2\cdot3}$ mW/cm^2 a large oscillation following the peak and preceding the plateau can be seen even at this slow sweep speed as a thickening of the initial rising phase trace.

Absence of demonstrable electrical coupling between receptor cells

The photoreceptors of the lateral eye of another barnacle species, *B. eburneus*, are electrically coupled to one another (Brown, Hagiwara, Koike & Meech, 1971; Shaw, 1972). We searched for evidence of electrical coupling

between receptor cells of the median ocellus by impaling simultaneously the cell bodies or axons of two photoreceptors with two micro-electrodes (Text-fig. 8).

In one series of experiments, electrodes were placed in adjacent, visually distinct receptor somata or axons. Coupling between the two electrodes was sought by passing through one of them currents sufficient to cause up to an 80 mV hyperpolarization or a 30 mV depolarization (1–5 nA; depolarizing currents cause smaller changes in membrane potential per

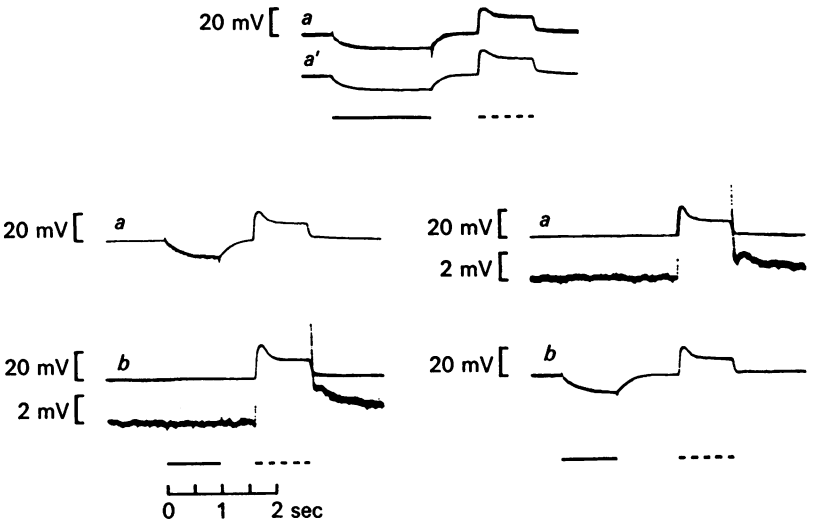

Text-fig. 8. Absence of significant electrical coupling between two visually distinct photoreceptor axons. The upper pair of traces shows both electrodes situated in one receptor (cell *a*). A hyperpolarizing current pulse (solid bar) is injected into the cell through one electrode which, by the use of a bridge circuit, is also employed to measure potential (upper trace). A second electrode placed nearby in the same cell records a similar potential change (lower trace). The lower sets of traces show results with the electrodes situated in two adjacent axons (cells *a* and *b*). On the left, current passed into receptor *a* causes no detectable voltage change in receptor *b*, shown at both low and high gains. In the reciprocal experiment on the right, current injected into receptor *b* elicits no potential change in receptor *a*. A light stimulus of $10^{-2\cdot9}$ mW/cm^2 (dotted bar) elicits a comparable photoresponse in each receptor.

nA because of membrane rectification); potential changes above the noise level of 0·2 mV were sought at the second electrode. In sixteen out of seventeen simultaneous impalements of visually distinct receptor cells with good photoresponses, current did not pass between the cells in either the hyperpolarizing or the depolarizing direction. Consequently, if electrical

coupling exists between these cells, its ratio must be less than about 1:150 for hyperpolarizing pulses or 1:60 for depolarizing pulses. Note that this ratio will be accurate only if the voltage recorded at the current-passing electrode by way of a bridge circuit is accurate. Often the bridge balance was tested by placing both electrodes in one cell, balancing the bridge of one electrode and recording the true voltage change with the other (Text-fig. 8). In one experiment, two visually distinct receptor cells appeared to be coupled, but it is possible that one of the electrodes passed through a dendrite of one cell before it impaled the other and created an artifical channel between them. Alternatively, both electrodes could have been located in the same receptor, one in the soma and the second in a dendrite at some distance from the cell.

In a separate series of experiments, a soma was penetrated and then all four of the visually distinct receptor axons some distance along the ocellar nerve were impaled sequentially with a second electrode. Only when the axonal electrode was in a specific one of the four axons did it record a voltage change when current was passed out of the electrode located in the soma. This was true regardless of whether the pulses were depolarizing or hyperpolarizing. We conclude that significant electrical coupling does not exist among these receptor neurones, and that it is therefore possible to know when two electrodes are located in the same cell because only then will currents passed through one electrode be recorded by the other. In support of these conclusions, we observed that when electrodes were located in two cells judged to be distinct because current did not pass between them, the time courses of the post-illumination hyperpolarizations they recorded were slightly different. When the electrodes were judged by current pulses to be located in the same cell, the time courses of these hyperpolarizations were indistinguishable.

DISCUSSION

The photoreceptor cells of the median ocellus of the giant barnacle are unique because their large size enables one to view them throughout their entire length under the dissecting microscope. This feature permits intracellular recording from the cells' somata, from their axons, and from visible axon terminal branches 99% of the distance from the light-sensitive dendrites to the presynaptic terminals. The large diameters of the four receptor axons of the ocellar nerve, and of their terminal branches in the ganglionic commissure, make them readily identifiable in thin sections, a feature which facilitates correlated studies of the fine structures of their somata, axons, and synaptic regions.

In their response to flashes and long pulses of light, the receptor cells of

the median ocellus show a remarkable similarity to the well-characterized retinular cells of the honeybee drone (Baumann, 1968). The shape and time course of the peak and plateau depolarizations are similar as well to those of the photoreceptors of other barnacles and of numerous other invertebrate species (Naka, 1961; Millecchia & Mauro, 1969; Shaw, 1967; Ioannides & Walcott, 1971; Järvilehto & Zettler, 1971; Chappell & Dowling, 1972). In addition, the fine structure of the presynaptic terminals of the receptor cells is similar to that of synaptic endings of other arthropod photoreceptor neurones. The characteristic apposition of the presynaptic site to two post-synaptic processes, presynaptic dense structure at the point at which the three cells meet, and widened intercellular cleft between the presynaptic and post-synaptic cells, have all been seen in synapses made by receptors from a number of other arthropods (Trujillo-Cenóz, 1965*a*,*b*; Dowling & Chappell, 1972). One feature of other arthropod receptor cell synapses not yet observed in the terminals of barnacle receptor neurones is the reciprocal contact from post-synaptic cells back onto receptor processes (Dowling & Chappell, 1972). Our failure to find such contacts may indicate that there is no feed-back at this level in the median visual pathways of the barnacle, or may suggest that the contacts appear on a different region of the presynaptic arborization from that which we have searched. We have also not observed synaptic contacts among the receptor cells, at their terminals or elsewhere, which complements the physiological finding that these cells are not electrically coupled to one another.

Because there is no demonstrable electrical coupling between photoreceptors of the median ocellus of the giant barnacle, one can place two electrodes into a receptor cell and be confident that both are in the same cell. Thus, with one electrode in the soma and another at some distance down the axon, one can analyse the decay of the visual response along the cell (Hudspeth *et al.* 1977); the current flowing across the cell's membrane as a consequence of either illumination or injection through a microelectrode does not spread to other photoreceptors.

In the visual systems of both vertebrates and invertebrates, photoreceptors with similar properties tend to be coupled. Vertebrate rods (Schwartz, 1973, 1975; Copenhagen & Owen, 1976) and cones (Baylor, Fuortes & O'Brien, 1971), and various invertebrate photoreceptors (Borsellino, Fuortes & Smith, 1965; Shaw, 1969; Muller, 1973) including those of the lateral eye of the barnacle *B. eburneus* (Brown *et al.* 1971; Shaw, 1972) are coupled to one another. Receptors which differ in properties such as sensitivity to a specific plane of polarized light or spectral sensitivity are usually not significantly coupled even though they be within the same eye (Shaw, 1967; Baylor & Hodgkin, 1973; Muller, 1973). Since the photoreceptors of the barnacle median eye appear similar to

one another, the absence of coupling between them was unexpected. We do not know if this absence of coupling is functionally significant, or if the receptor cells of the lateral eye of the giant barnacle are coupled as in *B. eburneus*. Since the median and lateral eyes lie in different positions within the animal and probably receive different information concerning light, they could serve different functions.

Shaw (1972) has demonstrated that the visual signals of the lateral photoreceptors of *B. eburneus* spread down their axons with relatively little attenuation. This is also the case for the median receptor cells of the giant barnacle. We have observed that large depolarizations are severely attenuated at the terminal region, presumably because of membrane rectification. Shaw also observed this phenomenon in the terminals of the receptors of the lateral eye (Shaw, 1972, Fig. 9*B*); in his figure there is no peak depolarization, and a train of light pulses that depolarized the cell to a 14 mV plateau hyperpolarized the cell by 22 mV at the termination of the illumination. Thus, in these decrementally conducting receptor cells, the range of voltage changes in the presynaptic region which might influence post-synaptic cells differs considerably from that generated by light in the receptor soma.

The authors thank Dr S. Hagiwara for advice and support to A.E.S. during initial experiments and Dr M. Poo for participating in experiments on electrical coupling. We are grateful to Messrs D. Corey, J. Gagliardi and P. Koen and Ms L. Yu for technical and photographic assistance, to Drs B. Forslind, U. McMahan and J.-P. Revel for the use of electron microscopes and to Mr D. Edgington and Drs C. Bader, J. E. Brown and S. W. Kuffler for comments on the manuscript. This study was supported by N.I.H. grants EY-01188 and EY-70985 to A.E.S. and by grants from the Merck Company Foundation and the Alfred P. Sloan Foundation to A.J.H.

REFERENCES

BADER, C. R., BAUMANN, F. & BERTRAND, D. (1976). Role of intracellular calcium and sodium in light adaptation in the retina of the honeybee drone (*Apis mellifera*, L.). *J. gen. Physiol.* **67**, 457–491.

BAUMANN, F. (1968). Slow and spike potentials recorded from retinula cells of the honeybee drone in response to light. *J. gen. Physiol.* **52**, 855–875.

BAUMANN, F. & HADJILAZARO, B. (1972). Depolarizing aftereffect of intense light in the drone visual receptor. *Vision Res.* **12**, 17–31.

BAYLOR, D. A., FUORTES, M. G. F. & O'BRYAN, P. M. (1971). Receptive fields of cones in the retina of the turtle. *J. Physiol.* **214**, 265–294.

BAYLOR, D. A. & HODGKIN, A. L. (1973). Detection and resolution of visual stimuli by turtle photoreceptors. *J. Physiol.* **234**, 163–198.

BORSELLINO, A., FUORTES, M. G. F. & SMITH, T. G. (1965). Visual responses in *Limulus*. *Cold Spring Harb. Symp. quant. Biol.* **30**, 429–443.

BROWN, J. E. & LISMAN, J. E. (1972). An electrogenic sodium pump in *Limulus* ventral photoreceptor cells. *J. gen. Physiol.* **59**, 720–733.

BROWN, H. M., HAGIWARA, S., KOIKE, H. & MEECH, R. M. (1970). Membrane properties of a barnacle photoreceptor examined by the voltage clamp technique. *J. Physiol.* **208**, 385–413.

BROWN, H. M., HAGIWARA, S., KOIKE, H. & MEECH, R. W. (1971). Electrical characteristics of a barnacle photoreceptor. *Fedn Proc.* **30**, 69–78.

CHAPPELL, R. L. & DOWLING, J. E. (1972). Neural organization of the median ocellus of the dragonfly. I. Intracellular electrical activity. *J. gen. Physiol.* **60**, 121–147.

CORNWALL, I. E. (1953). The central nervous system of barnacles (Cirripedia). *J. Fish. Res. Bd. Can.* **10**, 76–84.

COPENHAGEN, D. R. & OWEN, W. G. (1976). Coupling between rod photoreceptors in a vertebrate retina. *Nature, Lond.* **260**, 57–59.

DOWLING, J. E. & CHAPPELL, R. L. (1972). Neural organization of the median ocellus of the dragonfly. II. Synaptic structure. *J. gen. Physiol.* **60**, 148–165.

FAHRENBACH, W. H. (1965). The micromorphology of some simple photoreceptors. *Z. Zellforsch. mikrosk. Anat.* **66**, 233–254.

FULPIUS, R. & BAUMANN, F. (1969). Effects of sodium, potassium and calcium ions on slow and spike potentials in single photoreceptor cells. *J. gen. Physiol.* **53**, 541–561.

FUORTES, M. G. F. & YEANDLE, S. (1964). Probability of occurrence of discrete potential waves in the eye of *Limulus*. *J. gen. Physiol.* **47**, 443–463.

GWILLIAM, G. F. (1963). The mechanism of the shadow reflex in Cirripedia. I. Electrical activity in the supraoesophageal ganglion and ocellar nerve. *Biol. Bull. mar. biol. Lab., Woods Hole* **125**, 470–485.

GWILLIAM, G. F. (1965). The mechanism of the shadow reflex in Cirripedia. II. Photoreceptor cell response, second-order responses, and motor cell output. *Biol. Bull. mar. biol. Lab., Woods Hole* **129**, 244–256.

GWILLIAM, G. F. (1976). The mechanisms of the shadow reflex in Cirripedia. III. Rhythmical patterned activity in central neurons and its modulation by shadows. *Biol. Bull. mar. biol. Lab., Woods Hole* **151**, 141–160.

GWILLIAM, G. F. & BRADBURY, J. C. (1971). Activity patterns in the isolated central nervous system of the barnacle and their relation to behaviour. *Biol. Bull. mar. biol. Lab., Woods Hole* **141**, 502–513.

HAGINS, W. A. (1965). Electrical signs of information flow in photoreceptors. *Cold Spring Harb. Symp. quant. Biol.* **30**, 403–418.

HAGINS, W. A., PENN, R. D. & YOSHIKAMI, S. (1970). Dark current and photocurrent in retinal rods. *Biophys. J.* **10**, 380–412.

HUDSPETH, A. J., POO, M. M. & STUART, A. E. (1977). Passive signal propagation and membrane properties in median photoreceptors of the giant barnacle. *J. Physiol.* **272**, 25–43.

IOANNIDES, A. C. & WALCOTT, B. (1971). Graded illumination potentials from retinula cell axons in the bug, *Lethocerus*. *Z. vergl. Physiol.* **71**, 315–325.

JÄRVILEHTO, M. & ZETTLER, F. (1971). Localized intracellular potentials from pre- and postsynaptic components in the external plexiform layer of an insect retina *Z. vergl. Physiol.* **75**, 422–440.

KOIKE, H., BROWN, H. M. & HAGIWARA, S. (1971). Hyperpolarization of a barnacle photoreceptor membrane following illumination. *J. gen. Physiol.* **57**, 723–737.

KUSHIDA, H. (1971). A new method for embedding with Epon 812. *J. Electron. Microsc. Chiba Cy* **20**, 206–207.

LISMAN, J. E. & BROWN, J. E. (1972). The effects of intracellular iontophoretic injection of calcium and sodium ions on the light response of *Limulus* ventral photoreceptors. *J. gen. Physiol.* **59**, 701–719.

LISMAN, J. E. & BROWN, J. E. (1975). Light-induced changes of sensitivity in *Limulus* ventral photoreceptors. *J. gen. Physiol.* **66**, 473–488.

LUFT, J. H. (1961). Improvements in epoxy resin embedding methods. *J. biophys. biochem. Cytol.* **9**, 409–414.

MCMAHAN, U. J. & KUFFLER, S. W. (1971). Visual identification of synaptic boutons on living ganglion cells and of varicosities in postganglionic axons in the heart of the frog. *Proc. R. Soc.* B **177**, 485–508.

MILLECCHIA, R. & GWILLIAM, G. F. (1972). Photoreception in a barnacle: electrophysiology of the shadow reflex pathway in *Balanus cariosus*. *Science, N.Y.* **177**, 438–441.

MILLECCHIA, R. & MAURO, A. (1969). The ventral photoreceptor cells of *Limulus*. II. The basic photoresponse. *J. gen. Physiol.* **54**, 310–351.

MULLER, K. J. (1973). Photoreceptors in the crayfish compound eye: electrical interactions between cells as related to polarized light sensitivity. *J. Physiol.* **232**, 573–595.

NAKA, K.-I. (1961). Recording of retinal action potentials from single cells in the insect compound eye. *J. gen. Physiol.* **44**, 571–584.

OZAWA, S., HAGIWARA, S., NICHOLAYSEN, K. & STUART, A. E. (1976). Signal transmission from photoreceptors to ganglion cells in the visual system of the giant barnacle. *Cold Spring Harb. Symp. quant. Biol.* **40**, 563–570.

SCHWARTZ, E. A. (1973). Responses of single rods in the retina of the turtle. *J. Physiol.* **232**, 503–514.

SCHWARTZ, E. A. (1974). Responses of bipolar cells in the retina of the turtle. *J. Physiol.* **236**, 211–224.

SCHWARTZ, E. A. (1975). Rod–rod interaction in the retina of the turtle. *J. Physiol.* **246**, 617–638.

SHAW, S. R. (1967). Simultaneous recording from two cells in the locust retina. *Z. vergl. Physiol.* **55**, 183–194.

SHAW, S. R. (1969). Interreceptor coupling in ommatidia of drone honeybee and locust compound eyes. *Vision Res.* **9**, 999–1029.

SHAW, S. R. (1972). Decremental conduction of the visual signal in barnacle lateral eye. *J. Physiol.* **220**, 145–175.

TRUJILLO-CENÓZ, O. (1965*a*). Some aspects of the structural organization of the arthropod eye. *Cold Spring Harb. Symp. quant. Biol.* **30**, 371–382.

TRUJILLO-CENÓZ, O. (1965*b*). Some aspects of the structural organization of the intermediate retina of dipterans. *J. Ultrastruc. Res.* **13**, 1–33.

VENABLE, J. H. & COGGESHALL, R. (1965). A simplified lead citrate stain for use in electron microscopy. *J. cell. Biol.* **25**, 407–408.

YEANDLE, S. (1958). Evidence of quantized slow potentials in the eye of the *Limulus*. *Am. J. Ophth.* **46**, 82–87.

ZETTLER, F. & JÄRVILEHTO, M. (1971). Decrement-free conduction of graded potentials along the axon of a monopolar neuron. *Z. vergl. Physiol.* **75**, 402–421.

EXPLANATION OF PLATES

PLATE 1

A, brightfield micrograph of a living experimental preparation from the giant barnacle, consisting of the median ocellus (MO), its median ocellar nerve (MON), and the supraoesophageal ganglion (SEG) in which the nerve terminates. Other processes of the ganglion include the paired lateral ocellar nerves (LON) and circumoesophageal connectives (CEC). Individual photoreceptor axons are visible within the median ocellar nerve (arrows). Scale, 1 mm.

B, Nomarski differential interference contrast micrograph of the median ocellus of a giant barnacle, demonstrating photoreceptor somata (coarse arrows) and their fine processes encapsulated by connective tissue. The axon of one receptor (fine arrow) is apparent as it enters the ocellar nerve. Scale, 50 μm.

C, light micrograph of a cross-section through a median ocellus, showing one photoreceptor cell with several of its irregular dendrites. The cell is surrounded by fine dendritic processes contributed by all four receptors and by the ocellar capsule. Scale, 50 μm.

D, Nomarski view of a living median ocellar nerve showing portions of three photoreceptor axons (arrows) and smaller accompanying fibres. Scale, 20 μm.

E, cross-section of the median ocellar nerve demonstrating the four large photoreceptor axons and numerous smaller fibres. While the majority of the small fibres are segregated within one compartment of the nerve, a few occur among the receptor axons. Scale, 20 μm.

F, Nomarski photomicrograph of two photoreceptor axons (arrows) entering the supraoesophageal ganglion and bifurcating; commissural fibres are evident in the lower portion of the Figure. Scale, 20 μm.

G, cross-section of the median ocellar nerve at its junction with the ganglionic commissure. Photoreceptor axons (arrows) are branching into finer processes which diverge into the two hemiganglia. Scale, 20 μm.

PLATE 2

A, high-magnification light micrograph of a median ocellar photoreceptor, showing its nucleus, two large masses of glycogen (arrows), and a single, stout dendrite terminating in a rhabdomere. The cell is surrounded by pigmented glial processes; a portion of the ocellar capsule is apparent at the left. Scale, 20 μm.

B, low-magnification electron micrograph showing dendritic processes within a median ocellus. The dendrites are filled with masses of glycogen (G) and clusters of mitochondria and lysosomes. The connective tissue capsule (C) is seen at the top of the Figure. Scale, 10 μm.

C, electron micrographic montage showing a short process extending from a photoreceptor soma (S) to end in a dendritic terminal (DT) filled with mitochondria and lysosomes and fringed with rhabdomeric microvilli. Two glial perikarya lie at the lower right of the field. Scale, 5 μm.

D, electron micrograph of four dendritic terminal bulbs transected at various levels to reveal the included organelles and closely packed microvilli. Scale, 2 μm.

E, high-power electron micrograph of a rhabdomere with a close-packed arrangement of microvilli and focal obliterations of the extracellular space. Scale, 0·2 μm.

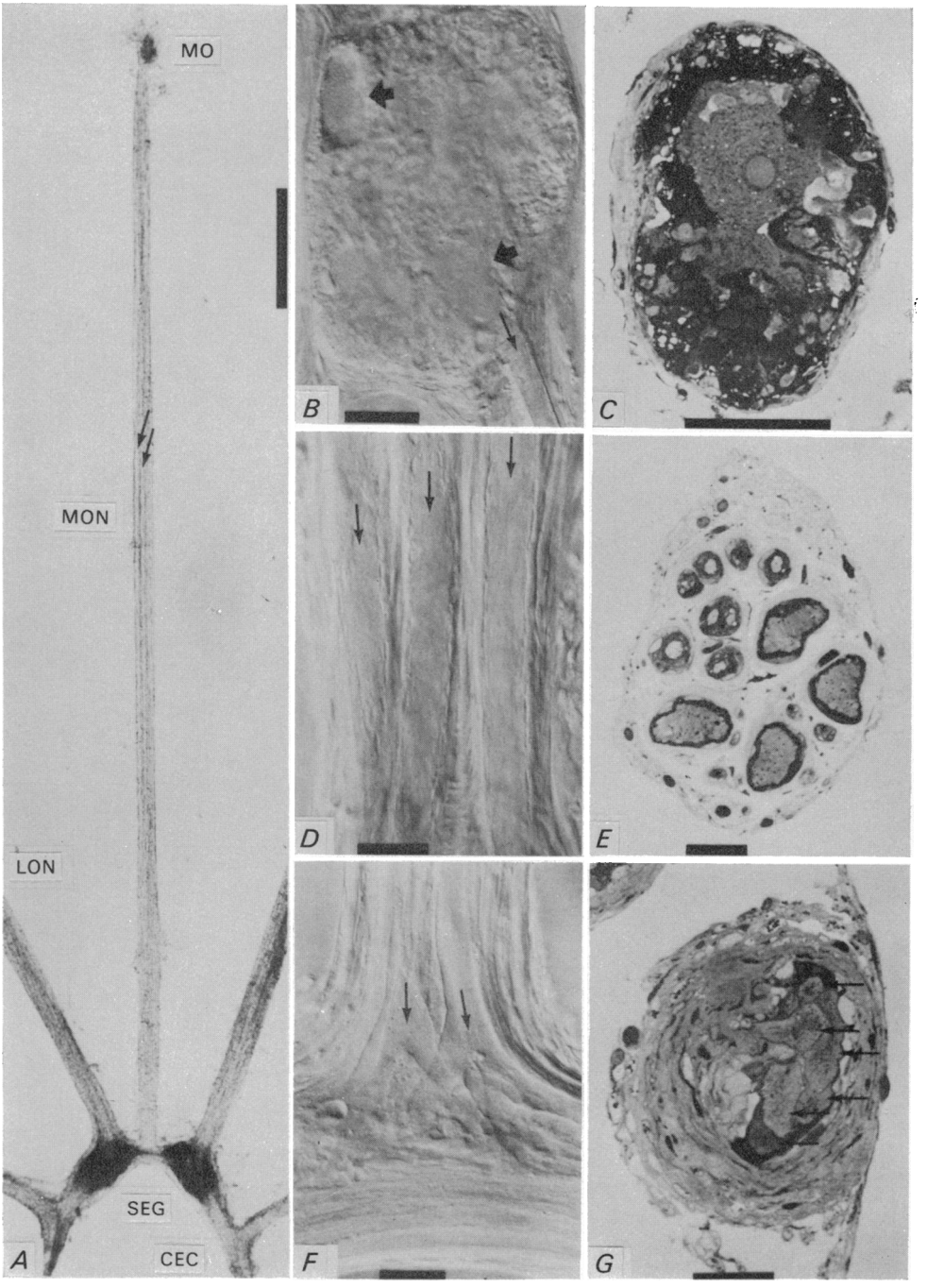
MO
MON
LON
SEG
CEC
A
B
C
D
E
F
G

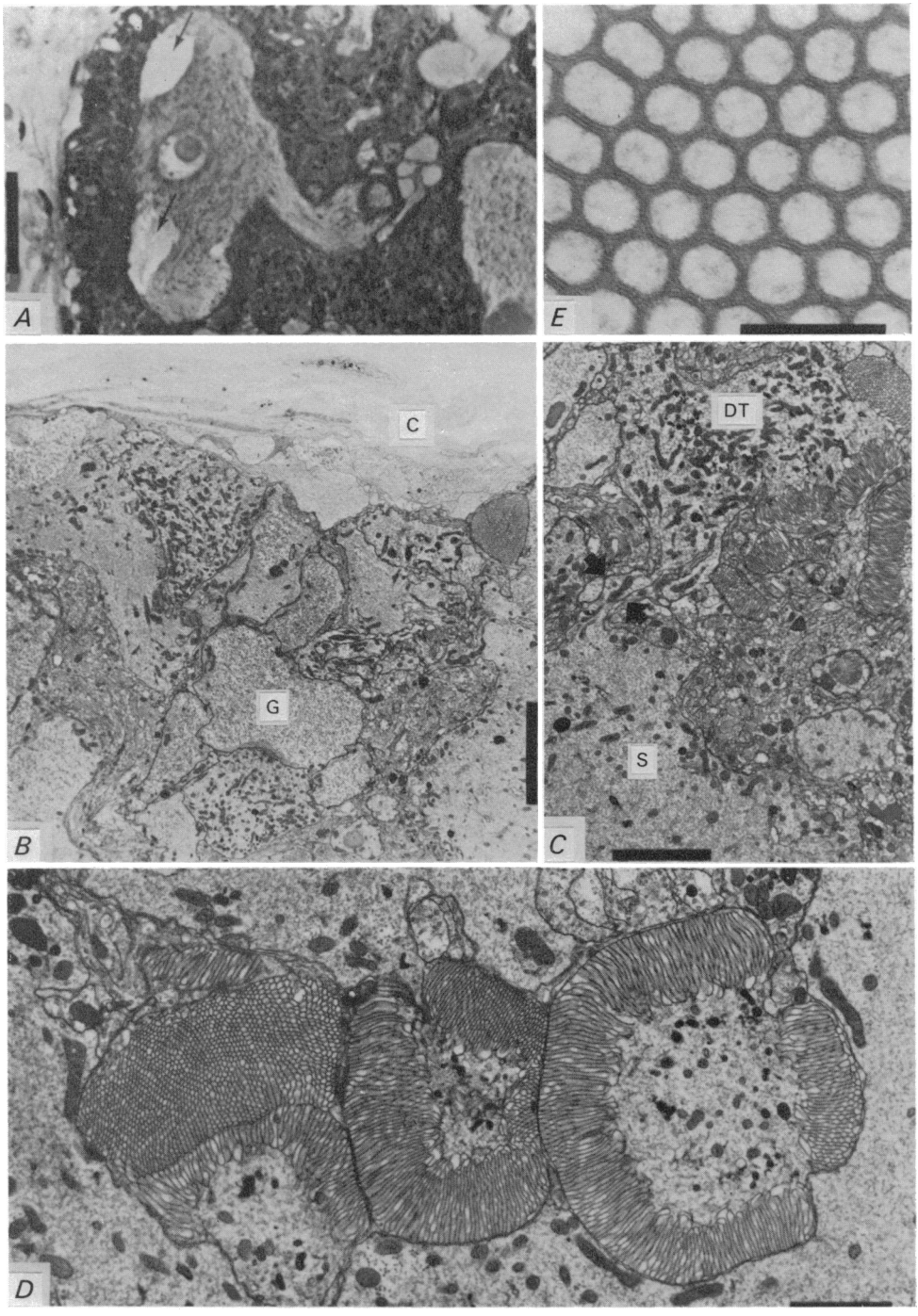
A
E
C
G
B
DT
S
C
D

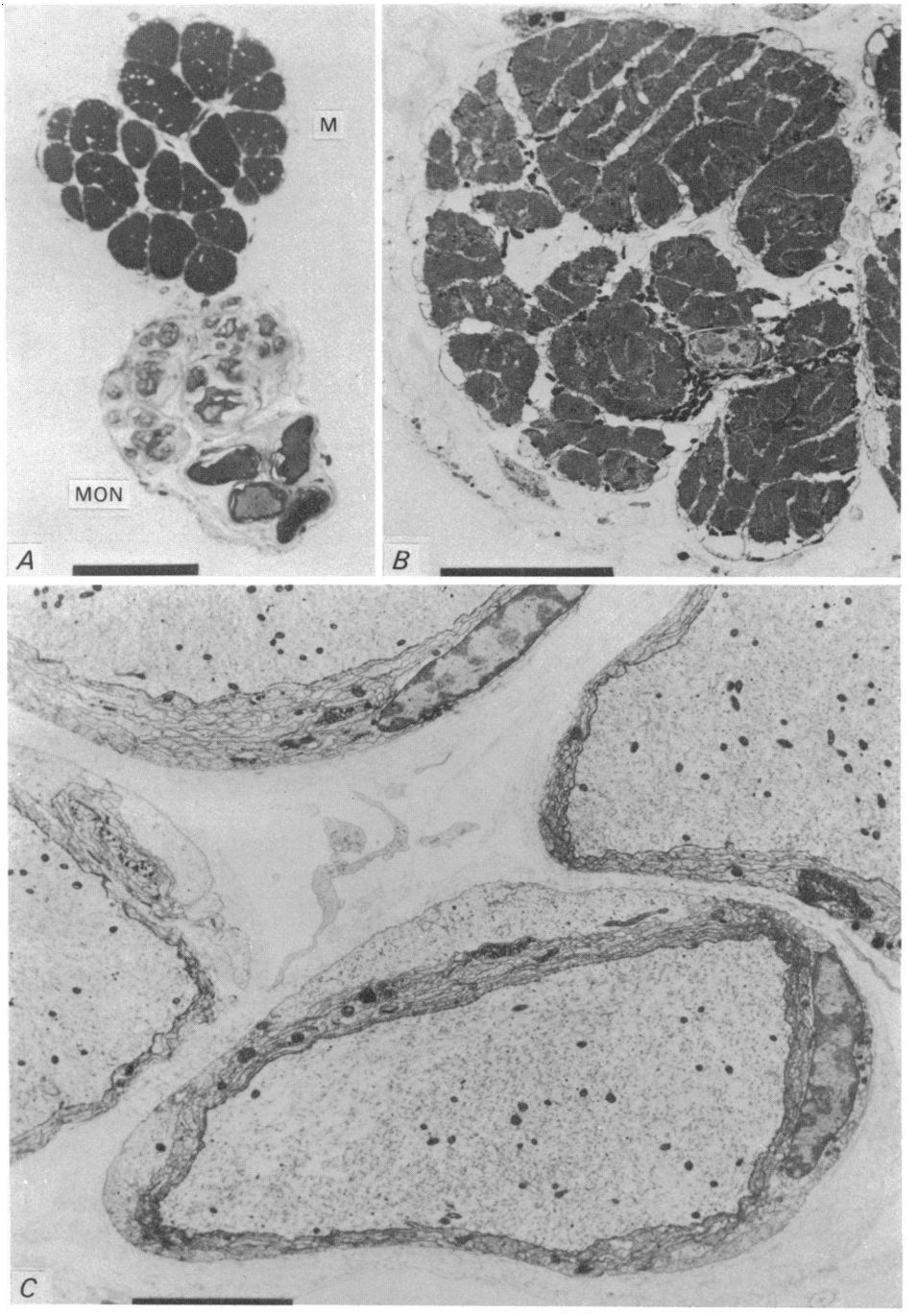
M
MON
A
B
C

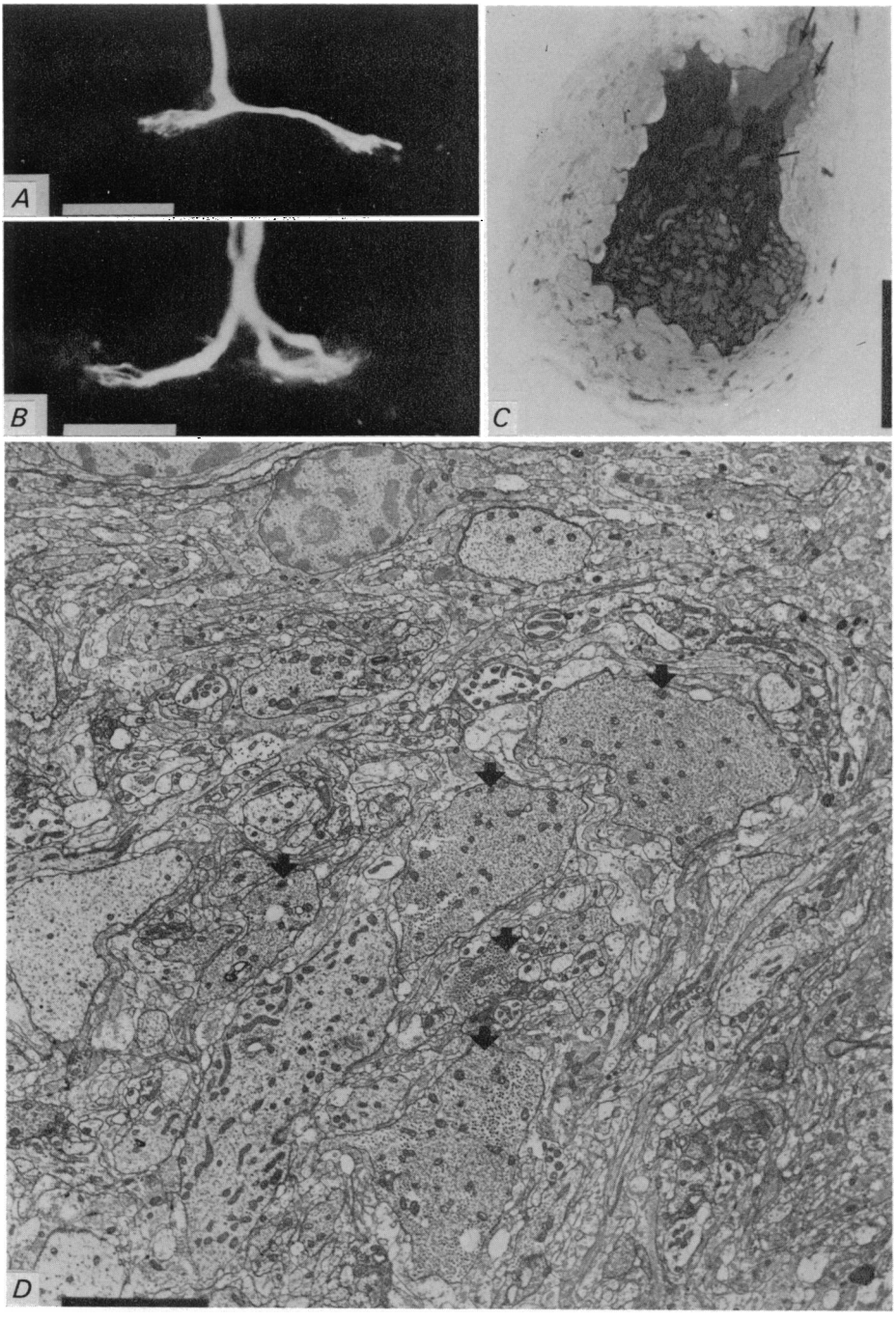

A. J. HUDSPETH AND A. E. STUART

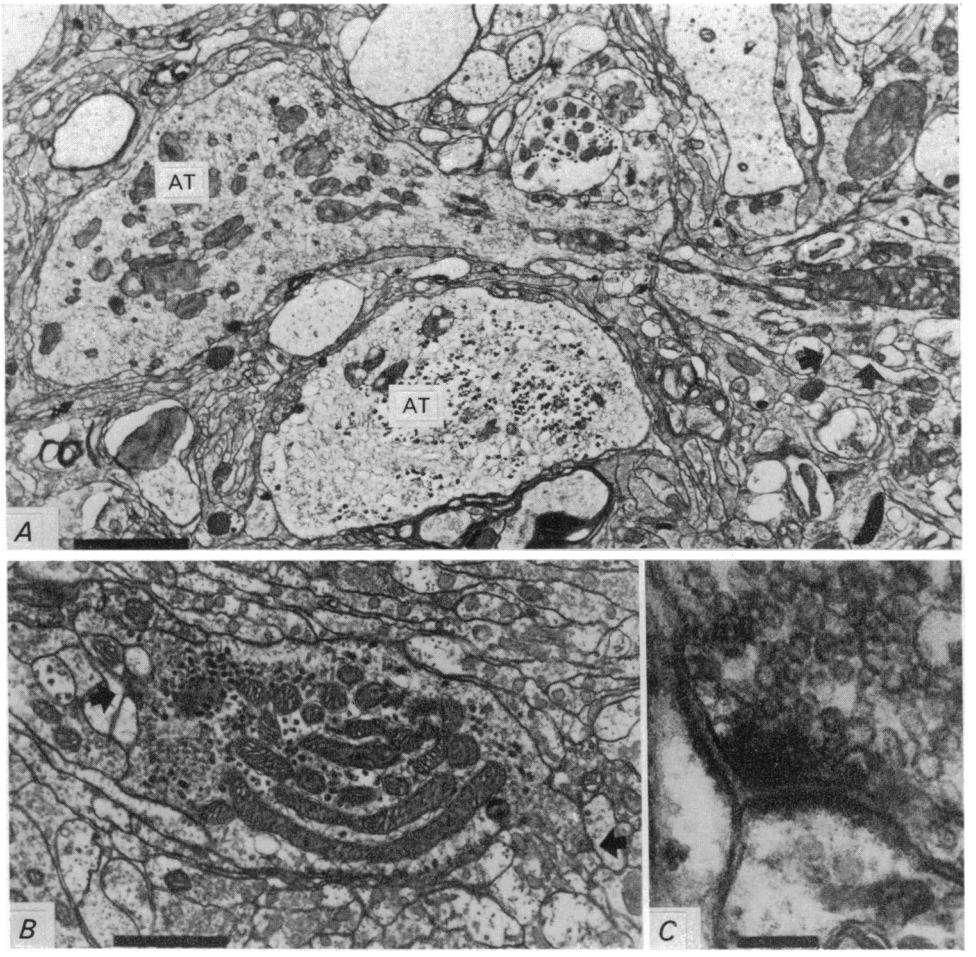
AT
AT
A
B
C

PLATE 3

A, photomicrograph of the median ocellar nerve (MON) and its associated muscular strand (M) in transverse section. The four photoreceptor axons, which are sectioned slightly obliquely, are segregated from smaller axons in the nerve by a connective tissue partition. Scale, 50 μm.

B, low-magnification electron micrograph showing that the small strand supporting the median ocellar nerve is a thin muscle with the large fibres characteristic of arthropods. Scale, 10 μm.

C, electron micrograph of portions of the four photoreceptor axons in transverse section. Each fibre is invested with several layers of wrapping by glial cells and surrounded by collagenous material. Scale, 5 μm.

PLATE 4

A, fluorescence photomicrograph of a Procion yellow-injected photoreceptor axon entering the supraoesophageal ganglion. This fibre forms a T-shaped branch by a simple bifurcation within the ganglionic commissure. Scale, 100 μm.

B, in this Procion yellow-injected preparation, the axon divides twice in Y-shaped junctions before it reaches the ganglion. Despite the complicated branching pattern, the axonal terminals within each hemiganglion are restricted to a small, roughly cylindrical region of neuropil. Scale, 100 μm.

C, photomicrograph of a sagittal section through the ganglionic commissure, demonstrating the segregation of the photoreceptor terminal processes (arrows) from the lighter-staining commissural fibres beneath. The axons lie within a matrix of pigmented glial cells and the entire ganglion is encapsulated by thick layers of connective tissue. Scale, 50 μm.

D, low-magnification electron micrograph of the commissural region, showing photoreceptor endings in the process of branching to form terminals. The axonal branches (arrows) which were followed from their parent axons in serial sections, are characterized by their glycogen content and relatively large size. Scale, 5 μm.

PLATE 5

A, electron micrograph of two axonal terminal processes (AT) of photoreceptors, traced in serial sections, showing their characteristic glycogen content and mitochondrial accumulation. The upper process extends a fine branch which is the site of several chemical synapses (arrows). Scale, 2 μm.

B, transverse electron microscopic section of a terminal photoreceptor branchlet showing two synaptic sites (arrows) with numerous associated synaptic vesicles. The process contains close-packed mitochondria and many dense, irregular, unbounded glycogen particles. Scale, 1 μm.

C, high-magnification electron micrograph showing a dyadic chemical synapse between an identified photoreceptor terminal branch (top) and two small postsynaptic elements. The synapse is characterized by the enlarged, regular intercellular space, pre- and post-synaptic membrane densities, and numerous membranous vesicles clustered about a presynaptic dense body. Scale, 0·2 μm.